

Electrochemical Immunoassay Determination of a Cancer Biomarker (CA19-9) by Horseradish Peroxidase

Songyan Zhang¹, Chengming Sun¹ and Wenping Zhou^{2,*}

¹ Department of Hepatopancreatobiliary Surgery, Harbin Medical University Cancer Hospital, Harbin 150040, China

² Department of Hepatobiliary Surgery, General Hospital of Shenyang Military, 83 Wenhua Road, Shenhe District, Shenyang 110016, Liaoning Province, China.

*E-mail: wenpingzhou_sunny@163.com

Received: 14 May 2017 / Accepted: 2 July 2017 / Published: 13 August 2017

This work developed an electrochemical immunosensor to quantitatively detect CA19-9 in human serum, a pancreatic cancer biomarker, where the electrode materials were thionine (TH) and graphene sheets (GS), and horseradish peroxidase (HRP) and ferroferric oxide (Fe₃O₄) nanoparticles-loaded mesoporous silica nanoparticles (MSNs) served as labels to amplify signals. The electron transfer and immobilization of primary antibody of CA19-9 (Ab₁) were enhanced by the as a substrate, the GS and TH hybrid (GS/TH). MSNs were used as a carrier for immobilization of secondary antibody of CA19-9 (Ab₂), Fe₃O₄, and HRP. The sensitivity of the immunosensor could be enhanced by the synergistic effect between HRP and Fe₃O₄. The proposed technique is potential to be applied to clinical analysis or be used to detect other tumor markers.

Keywords: Pancreatic cancer; Biomarker; Graphene; CA19-9; Horseradish peroxidase

1. INTRODUCTION

Koprowski reported a monoclonal antibody in 1979. This antibody was cultured from cells of colorectal carcinoma bound to antigenic determinants located on a sialylated Lewis A blood group oligosaccharide, and then he termed the antibody serum carbohydrate antigen 19-9 (CA19-9) [1, 2]. Thus CA19-9 could not be synthesized in the 5% of the population who does not express the Lewis antibody [3]. There has been still relatively less studies on the clinical application of CA19-9 in pancreatic cancer diagnosis, meanwhile, meta-analysis has been considered essential to obtain meaningful results [4]. As shown in one meta-analysis of these previous works, the specificity toward pancreatic cancer at a CA19-9 level of 37 and 100 U/ml was 90 and 98%, respectively, whereas the

sensitivity at the same levels was 81 and 68%, respectively [5-9]. However, serum CA19-9 levels have been found to increase in an extensive range of benign and malignant conditions such as colorectal, hepatocellular, esophageal, lung, and ovarian carcinomas, cholangiocarcinoma, Hashimoto's thyroiditis, Sjögren's syndrome, heavy tea consumption, rheumatoid arthritis, inflammatory bowel disease, achalasia, pancreatitis, cirrhosis, hepatitis, choledocholithiasis, and cholecystitis [10-12].

CA19-9 has been in extensive use, though it has a range of drawbacks. Up till now, tumor markers like CA19-9 and morbid procedures including exploratory laparotomy have been used to diagnose pancreatic or biliary neoplasia considering the limitations in imaging. The discovery of CA19-9 in 1979 led to great improvement in the cross-sectional and endoscopic imaging and sampling, significantly enhancing the diagnosis capacity for diseases of the pancreas and bile ducts in a much less morbid way [13-15].

As bioanalytical tools, electrochemical immunosensors are portable, simple in fabrication, potential for mass – production, cost-effective, easy in use, and feasibly miniaturized. Thus they are considered as high-performance screening for biomolecule determination [16, 17]. Noise reduction and signal amplification are of vital importance to obtain low limit of detection (LOD) in clinical immunoassays [18-21]. Sandwich-type immunoassay uses a couple of match antibodies [22-24] as an extensively used protocol which is low in cost, acceptably selective, and easily miniaturized for ultrasensitive determination [25-27], thus this technique is highly specific and sensitive.

This study proposed a quantitative determination of CA19-9 using a sandwich electrochemical immunosensor based on a signal amplification technique, where the labels were horseradish peroxidase (HRP) and ferroferric oxide (Fe_3O_4) nanoparticles - loaded mesoporous silica nanoparticles (MSNs), and the sensing platform was thionine (TH) and graphene sheets (GS). GS is conductive, and possesses large surface area and ample functional groups, thus having become a research focus in electrochemical measurement [28-30]. TH has gained extensive use in analytical applications during the immunosensor fabrication as an electron transfer mediator [31, 32]. In addition, TH can be directly adsorbed onto GS via π - π stacking [33]. MSNs have the potential of being an excellent sensing material for electrochemical immunosensors as an outstanding good biological carrier because of its uniform structure and large surface area. Besides, Fe_3O_4 nanoparticles have some intrinsic good catalytic activity toward H_2O_2 . Therefore, HRP and Fe_3O_4 nanoparticles – loaded MSNs were considered to be used to synergistically amplify signal. Furthermore, besides the enhancement in electrochemical signal could be realized by HRP as a biological enzyme, HRP could also decrease the nonspecific adsorption (label – electrode surface). The aforementioned technique is potential to have application in clinical analysis or the determination of other tumor markers.

2. EXPERIMENTS

2.1. Chemicals

1-ethyl-3-(3-dimethylaminopropyl) carbodiimide (EDC), bovine serum albumin (BSA), Glutaraldehyde, and *N*-Hydroxysuccinimide (NHS) were commercially available in Sigma. The primary antibody of CA19-9 (Ab_1), secondary antibody of CA19-9 (Ab_2), and CA19-9 were

commercially available in Beijing Kwinbon Biotechnology. All other reagents were of analytical grade and used with no further purification. The electrolyte was phosphate-buffered saline (PBS) and used throughout. Ultrapure water was employed for the following electrochemical experiments.

2.2. Preparation of amino-functionalized MSNs

The synthesis of MSNs was performed using the method proposed by Zhao et al. [34]. After dissolution in the absolute ethanol (15 ml), the synthesized MSNs were transferred to a three-necked flask (100-ml), heated to 70 °C and magnetically stirred. Then (3-aminopropyl)triethoxysilane (APTES) (50 μ l) was added, then kept at 70 °C for 3 h. The mixture was then centrifuged, washed using absolute ethanol, and dried at ambient temperature in high vacuum for 12 h to yield the terminal amino-functionalized MSNs.

2.3. Preparation of bromine-functionalized Fe_3O_4

Fe_3O_4 nanoparticles were synthesized using the previously proposed technique [35]. Subsequently, 2-bromo-2-methyl-propionic acid (1.6633 g) and citric acid (0.1668 g) were dissolved in *N,N*-dimethylformamide (DMF) and chloroform mixture (volume 1:1). The obtained mixture was diluted to 50 ml. 30 ml solution was taken out of this mixed solution and introduced to Fe_3O_4 . The mixture was kept at 30 °C under agitation overnight, and then centrifuged, washed and dried to obtain the bromine-functionalized Fe_3O_4 nanoparticles.

2.4. Preparation of Fe_3O_4 -MSN-HRP- Ab_2 conjugation

After dispersing aliquot of Fe_3O_4 and MSNs nanoparticles in ethanol under agitation overnight, the obtained products were centrifuged successively using ethanol and ultrapure water, redispersed in ultrapure water. This was followed incubating these products in glutaraldehyde solution for 120 min. Then they were centrifuged and washed to obtain the Fe_3O_4 -MSNs. Then the as-prepared hybrid was redispersed using 1 ml of PBS (2 mg/ml), followed by successive incubation in 1 ml of Ab_2 solution (10 μ g/ml) and 1 ml of HRP solution (100 μ g/ml) for 60 min to yield the Fe_3O_4 /MSN/HRP/ Ab_2 conjugation. After final centrifugation, the obtained mixture was washed using PBS, redispersed in PBS (1 ml) and stored at 4 °C before further use.

2.5. Preparation of CA19-9 immunosensor

After careful polishing using 1.0, 0.3, and 0.05 μ m Al_2O_3 powder respectively to mirror-like, glassy carbon electrode (GCE) was cleaned and left drying in air. The surface of this GCE was added with GS/TH solution (5 μ l), which was then left drying. This was followed by the immobilization of primary CA19-9 antibody (Ab_1) onto the aforementioned electrode surface, where an amidation reaction occurred between the accessible amine species of Ab_1 and the carboxylic acid species on GS.

This reaction was enhanced by the subsequent addition of EDC/NHS (3 μ l, 0.1 M). Then the electrode was washed. After incubation in BSA solution (1%) for 0.5 h to block nonspecific binding sites, this electrode went through incubation using CA19-9 solution at varied concentrations for 60 min, which was then dropped with the $\text{Fe}_3\text{O}_4/\text{MSN}/\text{HRP}/\text{Ab}_2$ solution. The modified electrode was then incubated for an additional 60 min, washed before further use. For comparison, this work prepared analogous immunosensors using $\text{Fe}_3\text{O}_4/\text{MSN}/\text{Ab}_2$ and $\text{MSN}/\text{HRP}/\text{Ab}_2$, respectively.

2.6. Characterization

Electrochemical experiments were carried out on a CHI 770 electrochemical workstation. A traditional triple-electrode configuration was employed throughout, where the working, reference and counter electrode were a GCE with a diameter of 4 mm, a saturated calomel electrode (SCE) and a platinum wire, respectively. A traditional electrochemical cell was used for all cyclic voltammetry (CV) measurements at a potential range of -0.6 to 0.6 V (vs. SCE) (sweeping rate: 100 mV/s) in pH 7.4 PBS before and after the addition of H_2O_2 (5 mM).

3. RESULTS AND DISCUSSION

Since electrochemical signal is produced from labels, the selection of them is of vital significance for the fabrication of sandwich electrochemical immunosensors. This work prepared three labels including $\text{MSN}/\text{Fe}_3\text{O}_4/\text{Ab}_2$, $\text{MSN}/\text{HRP}/\text{Ab}_2$, and $\text{MSN}/\text{Fe}_3\text{O}_4/\text{HRP}/\text{Ab}_2$ to fabricate electrochemical immunosensors. The CVs of the three immunosensors were compared in Figure 1. The catalytic substrate was H_2O_2 for the following experiment. With respect to these immunosensors, the optimal catalytic response to H_2O_2 was observed at the potential of -0.3 V, thus this potential was chosen for further experiment. An obvious catalytic characteristic appeared with a dramatic increase of the reduction current. This result indicated the immobilized HRP could retain high enzymatic catalytic activity [36]. The concentration for all the three labels was 2 mg/ml. The concentration of the CA19-9 was 1 ng/ml. A slight current variation of $0.6 \mu\text{A}$ was observed on the $\text{MSN}/\text{HRP}/\text{Ab}_2$ modified GCE, and $\text{MSN}/\text{Fe}_3\text{O}_4/\text{Ab}_2$ modified GCE showed a current variation of $1.5 \mu\text{A}$ (Figure 1). The $\text{MSN}/\text{Fe}_3\text{O}_4/\text{HRP}/\text{Ab}_2$ modified GCE showed the highest current variation of $4.9 \mu\text{A}$, even higher than the sum of the other two, indicating the appearance of a synergistic effect between HRP and Fe_3O_4 .

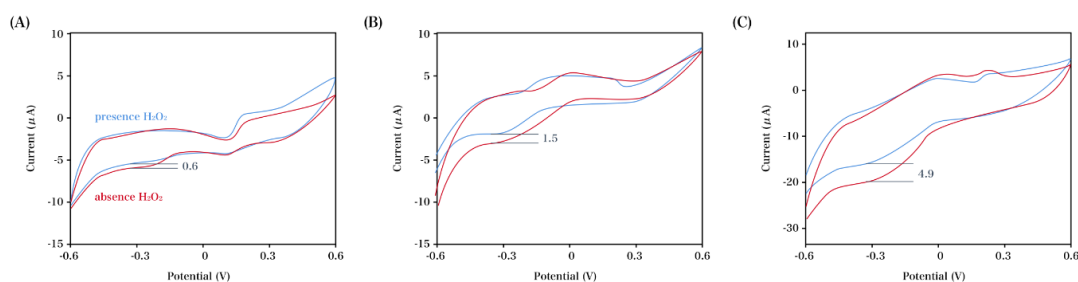


Figure 1. Electrochemical responses to H_2O_2 at varied electrodes: (A) $\text{MSN}/\text{HRP}/\text{Ab}_2/\text{GCE}$; (B) $\text{Fe}_3\text{O}_4/\text{MSN}/\text{Ab}_2/\text{GCE}$; (C) $\text{Fe}_3\text{O}_4/\text{MSN}/\text{HRP}/\text{Ab}_2/\text{GCE}$.

Figure 2 showed the comparison of varied electrodes to work out the benefits of our proposed immunoassay, where a high current was observed on the $\text{Fe}_3\text{O}_4/\text{MSN}/\text{HRP}/\text{Ab}_2$ modified GCE. $\text{Fe}_3\text{O}_4/\text{MSN}/\text{HRP}/\text{Ab}_2$ and HRP/Ab_2 , the secondary antibodies were also used as probes during the investigation of the effect of the $\text{Fe}_3\text{O}_4/\text{MSN}/\text{HRP}$ on the sensitivity of the measurement. Initially, the immunosensors of the same batch were used using the same concentration of CA 19-9. Subsequently, other two probes were employed. Compared with the response and sensitivity obtained using $\text{HRP}/\text{anti-CA 19-9}$ as the recognition element, that of the $\text{Fe}_3\text{O}_4/\text{MSN}/\text{HRP}/\text{Ab}_2$ was more pronounced, possibly due to the potential significant enhancement in the immobilization density of thionine and Ab_2 by the high surface-to-volume ratio (S/V) of graphene- Fe_3O_4 . During this process, the electron transfer from the base electrode surface to the redox center of HRP could be favorably enhanced by the thionine as a desirable mediator, where a large amount of HRP molecules were captured into the electrode. During the reaction between the antibody molecule bound onto the HRP surface and the corresponding antigen, the carried HRP molecules showed a higher catalytic efficiency relative to the thionine and H_2O_2 system compared with that only using HRP-labeled secondary antibody. This was mainly attributed to the fact that the big protein immobilized on the surface of the electrode prohibits the electron transfer from the solution to the surface of the electrode [37]. Therefore, thousands of HRP were loaded by the $\text{Fe}_3\text{O}_4/\text{MSN}$, enhancing the sensitivity of our developed immunosensor towards CA 19-9.

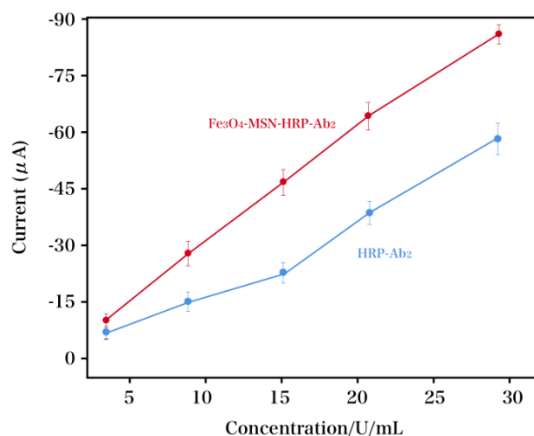


Figure 2. Amperometric responses of the immunosensor to CA 19-9 with varied concentrations: $\text{Fe}_3\text{O}_4/\text{MSN}/\text{HRP}/\text{Ab}_2$ modified GCE and HRP/Ab_2 modified GCE in PBS + 10.0 mM H_2O_2 .

The increase in the number of HRP molecules encapsulated in the liposomes led to the initial signal amplification. It is obvious that the increase in the amount of HRP encapsulated in the $\text{Fe}_3\text{O}_4/\text{MSN}$ caused enhanced sensitivity of the electrochemical immunosensor. Therefore HRP with a concentration range of 10 to 200 $\mu\text{g}/\text{mL}$ was used for the optimization of the encapsulation of HRP within $\text{Fe}_3\text{O}_4/\text{MSN}$. The CA 19-9 was determined using the electrochemical immunosensor based on a range of anti-CA 19-9 antibody-coated $\text{Fe}_3\text{O}_4/\text{MSN}$ encapsulated with HRP (varied concentrations). With the variation in the concentrations of HRP from 10 to 200 $\mu\text{g}/\text{mL}$, there was a significant decrease in the stripping peak. As the HRP concentration increased beyond 200 $\mu\text{g}/\text{mL}$, there was no pronounced decrease. The high signal amplification of the $\text{Fe}_3\text{O}_4/\text{MSN}/\text{HRP}/\text{Ab}_2$ modified GCE

bioconjugate may be attributed to the synergistic action of $\text{Fe}_3\text{O}_4/\text{MSN}$ and HRP could extremely amplify the electrochemical signal [38]. Therefore, 200 $\mu\text{g}/\text{mL}$ was selected as the optimum HRP concentration for the preparation of liposomes in following experiments.

The pH value of the test solution was optimized to obtain the best electrochemical response for the immunoassay. The effect of PBS pH on CA 19-9 (20 U/mL) detection was shown in Figure 3. After incubation of at ambient temperature for 0.5 h in the incubation solution + CA 19-9 (5 μL , 20 U/mL) and $\text{Fe}_3\text{O}_4/\text{MSN}/\text{HRP}/\text{Ab}$ (5 μL), our proposed immunosensor was monitored by voltammetry in PBS buffer in the presence of 10.0 mM H_2O_2 at varied pH values. The current of the immunosensor indicated the effect. As shown in the test results, the current initially increase, and then decreased as the PBS pH increased. Nevertheless, the current response reached its best at pH 7.4, thus pH 7.4 was selected as the optimum pH value for the CA 19-9 determination.

Generally, the analytical features of the electrochemical immunoassay are usually affected by the incubation temperature and incubation time for the interaction between the antibody and antigen. Nevertheless, all tests were performed at ambient temperature considering their further application in real samples. The CA 19-9 (20 U/mL) was selected as the sample using varied incubation time at room temperature. As the incubation time increased, an increase in the cathodic currents as observed, which showed a tendency to decrease after 0.5 h. Hence 0.5 h was selected as the optimum incubation time for the interaction between the antibody and antigen.

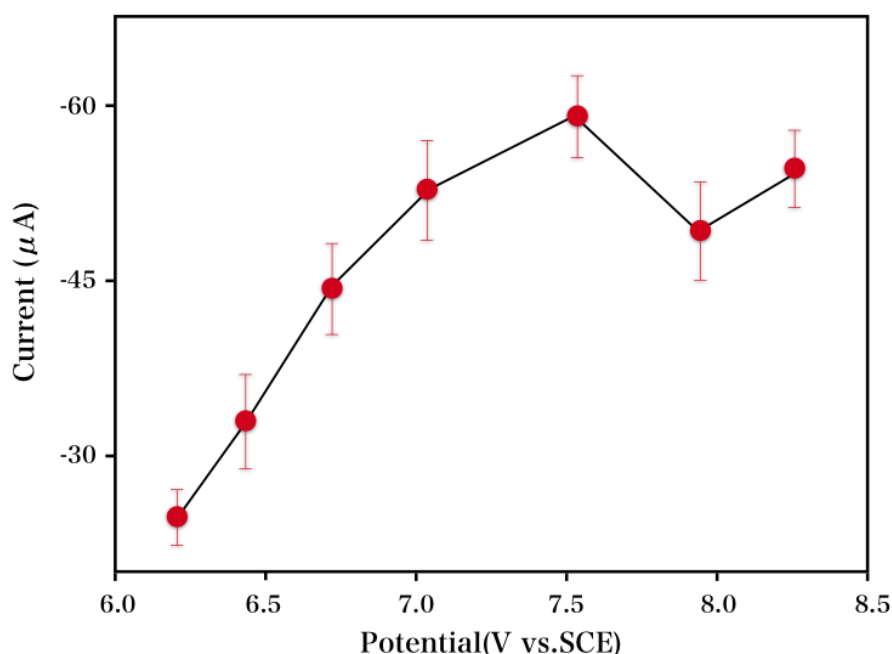


Figure 3. Effect of pH value on the detection of (20 U/mL) CA 19-9 in the presence of 10.0 mM H_2O_2 .

Under optimal conditions, as the CA 19-9 concentration in the incubation solution increased, a decrease in the differential pulse voltammetric (DPV) peak current of the as-prepared immunosensor was observed, as shown in Figure 4A. The same peak potential showed that the as-prepared

immunosensor was excellently reproducible. As indicated in the calibration plot in Figure 4B, a good linear relationship was found between the peak current, with the linear range of 2.0×10^{-5} to 40 U/mL and a correlation coefficient of 0.997. The LOD is 1.0×10^{-5} U/mL (S/N). The minimal concentration of analyte necessary to produce a characteristic signal at least 10-fold higher than the background noise is usually measured to obtain the limit of quantitation (LOQ), which is 1.6×10^{-5} U/mL in this case. The small error bars suggested the high precision of the signal responses, corresponding to the standard deviation (SD) of at least five measurements ($n \geq 5$) under each condition. The RSD ranges from 3.2 to 7.1%, indicating that the sensor preparation and the electrochemical assays were acceptably reproducible. As indicated in Table 1, the LOD and linear range of different sensors were compared. The comparison indicated a much lower LOD of the as-prepared biosensor. The encapsulated HRP obtained through the amplification method served as a label and enhance the sensitivity and the detectable concentration range to a large extent. As indicated by the above results, the as-prepared biosensor showed the optimum linear range and LOD, and had the potential of being applied to the CA 19-9 detection. The reproducibility of the proposed immunosensor was investigated by the intra- and inter-assays. All the relative standard deviations (RSD) for the intra- and inter-assay were not more than 3.9%. The experimental results suggested the acceptable reproducibility of the proposed immunosensor.

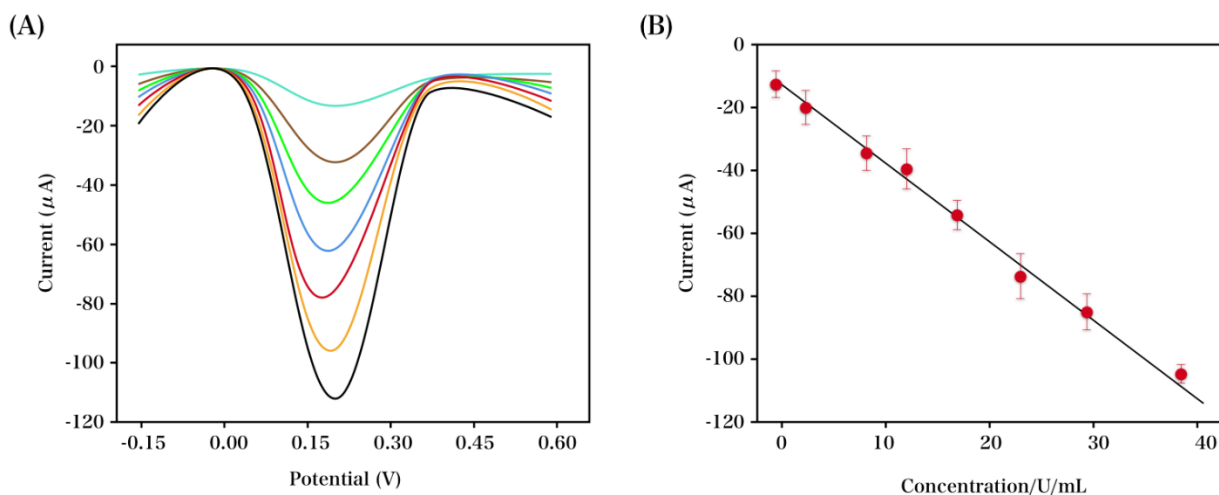


Figure 4. (A) DPV response of the immunosensor in PBS (pH 7.4, 0.2 M) + 10.0 mM H₂O₂ after incubation using CA 19-9 (0, 2.0×10^{-5} , 2.0×10^{-2} , 0.2, 2.0, 5.0, 15.0, 20.0, 25.0, 30.0, 40.0 U/mL) at decreasing peak currents. (B) Calibration profile of CA 19-9 immunoassay.

Table 1 Analytical characterization of varied CA 19-9 immunosensors and immunoassays.

Method	Linear range (U/mL)	LOD (U/mL)	Reference
Electrochemical immunosensor	2 to 30	1.4	[39]
Chemiluminescent immunosensor	2 to 25	1	[40]
Electrochemical immunosensor	3 to 20	2.68	[41]
Electrochemical immunosensor	0.1 to 180	0.04	[42]
Electrochemical immunosensor	0.15 to 150	0.06	[43]
Fe ₃ O ₄ -MSN-HRP-Ab ₂	0.0005 to 40	0.0001	This work

Clinical serum samples were collected from The Tumor Hospital Affiliated Harbin Medical University for further investigation of the analytical reliability and potential application of the as-prepared technique in real specimen detection. Note that the protocol has been validated by The Tumor Hospital Affiliated Harbin Medical University. This work compared the measurement results of CA 19-9 in human serum specimens obtained by our developed technique with the reference values using the purchased Electrochemiluminescent Analyzer (ROCHE E601, Switzerland). Before measurement, the serum specimens were successively diluted using PBS (1 mM, pH 7.4) for 10, and 100 times in the case of tumor marker levels higher than the maximum calibration ranges. Furthermore, the recovery experiments were performed by adding CA 19-9 in varied amounts into human serum specimens. As showed in Table 2, relative errors were observed below 4.41% for the determination of CA 19-9, with a recovery range of 94.7% to 104.2% for the CA 19-9 recovery test. These acceptable results indicated that our developed technique was accurate for the specimen determination. The results provided by the other two techniques agreed with the aforementioned results. Therefore, our developed immunosensor could be used for the preliminary CA 19-9 detection during clinical diagnosis.

Table 2. Application of the immunosensor in real specimens.

Sample	Found (U/mL)	RSD (%)	Recovery (%)	Reference value (U/mL)
1	4.52	0.98	101.12	4.47
2	22.14	3.88	98.84	22.40
3	7.98	2.54	101.78	7.84
4	12.40	4.41	101.47	12.22

4. CONCLUSIONS

This study proposed the fabrication of a new electrochemical immunosensor toward CA19-9 determination, where the substrate material was the GS/TH and the labels were HRP-and-Fe₃O₄ nanoparticles loaded MSNs. MSNs serve as an excellent carrier to immobilize secondary antibody, HRP and Fe₃O₄, since it was well biocompatible and possessed large specific surface area. The signal response was promoted by the synergistic effect between HRP and Fe₃O₄, due to their catalytic activity toward H₂O₂. Compared with the methods using single HRP and Fe₃O₄, this technique could provide enhanced signal and improve the sensitivity of our developed immunosensor.

ACKNOWLEDGEMENT

The work was supported by 2014 Science and Technology Research (Main) Project of Education Department of Heilongjiang Province, No.12541328.

References

1. H. Koprowski, Z. Steplewski, K. Mitchell, M. Herlyn, D. Herlyn and P. Fuhrer, *Somatic Cell and Molecular Genetics*, 5 (1979) 957.

2. J. Ramage, A. Donaghy, J.M. Farrant, R. Iorns and R. Williams, *Gastroenterology*, 108 (1995) 865.
3. M. Tempero, E. Uchida, H. Takasaki, D. Burnett, Z. Steplewski and P. Pour, *Cancer Research*, 47 (1987) 5501.
4. K. Goonetilleke and A. Siriwardena, *European Journal of Surgical Oncology (EJSO)*, 33 (2007) 266.
5. D. Parikh, B. Durbin-Johnson and S. Urayama, *Journal of Gastrointestinal Cancer*, 45 (2014) 74.
6. X. Yang, Y. Li, C. Chen, C. Peng, S. Liu and Y. Liu, *Medical Oncology*, 28 (2011) 789.
7. P. Wu, J. Zou, R. Tang, Y. Yao and C. You, *Chinese Journal of Cancer Research*, 23 (2011) 283.
8. M. Baine, M. Menning, L. Smith, K. Mallya, S. Kaur, S. Rachagani, S. Chakraborty, A. Sasson, R. Brand and S. Batra, *Cancer Biomarkers*, 11 (2012) 1.
9. Z. Yang, Y. Chevolut, Y. Ataman-Önal, G. Choquet-Kastylevsky, E. Souteyrand and E. Laurenceau, *Sensors and Actuators B: Chemical*, 175 (2012) 22.
10. A. Andriulli, T. Gindro, P. Piantino, R. Farini, G. Cavallini, L. Piazzi, R. Naccarato, G. Dobrilla, G. Verme and L.A. Scuro, *Digestion*, 33 (1986) 26.
11. O. Uygur-Bayramiçli, R. Dabak, E. Orbay, C. Dolapçioğlu, M. Sargın, G. Kılıçoğlu, Y. Güteryüzlü and A. Mayadağlı, *World J Gastroenterol*, 13 (2007) 5357.
12. A. Wannhoff, J. Hov, T. Folseraas, C. Rupp, K. Friedrich, J. Anmarkrud, K. Weiss, P. Sauer, P. Schirmacher and K. Boberg, *Journal of Hepatology*, 59 (2013) 1278.
13. H. Mertz, P. Sechopoulos, D. Delbeke and S. Leach, *Gastrointestinal Endoscopy*, 52 (2000) 367.
14. J. Sreenarasimhaiah, *Journal of Clinical Gastroenterology*, 42 (2008) 81.
15. G. Mishra and J. Conway, *Current Gastroenterology Reports*, 11 (2009) 150.
16. R. Elshafey, A.C. Tavares, M. Siaj and M. Zourob, *Biosensors and Bioelectronics*, 50 (2013) 143.
17. E. Bahadır and M. Sezgintürk, *Talanta*, 132 (2015) 162.
18. B. Zhang, B. Liu, G. Chen and D. Tang, *Biosensors and Bioelectronics*, 64 (2015) 6.
19. N. Liu, F. Feng, Z. Liu and Z. Ma, *Microchim. Acta.*, 182 (2015) 1143.
20. H. Ilkhani, M. Sarparast, A. Noori, S. Bathaie and M.F. Mousavi, *Biosensors and Bioelectronics*, 74 (2015) 491.
21. A. Ravalli, C. da Rocha, H. Yamanaka and G. Marrazza, *Bioelectrochemistry*, 106 (2015) 268.
22. K. Tawa, F. Kondo, C. Sasakawa, K. Nagae, Y. Nakamura, A. Nozaki and T. Kaya, *Anal. Chem.*, 87 (2015) 3871.
23. H. Jia, P. Gao, H. Ma, D. Wu, B. Du and Q. Wei, *Bioelectrochemistry*, 101 (2015) 22.
24. X. Wang, C. Chu, L. Shen, W. Deng, M. Yan, S. Ge, J. Yu and X. Song, *Sensors and Actuators B: Chemical*, 206 (2015) 30.
25. P. Jolly, N. Formisano and P. Estrela, *Chemical Papers*, 69 (2015) 77.
26. E. Arkan, R. Saber, Z. Karimi and M. Shamsipur, *Anal. Chim. Acta.*, 874 (2015) 66.
27. Y. Li, J. Han, R. Chen, X. Ren and Q. Wei, *Analytical Biochemistry*, 469 (2015) 76.
28. J. Liu, J. Wang, T. Wang, D. Li, F. Xi, J. Wang and E. Wang, *Biosensors and Bioelectronics*, 65 (2015) 281.
29. H. Chou, C. Fu, C. Lee, N. Tai and H. Chang, *Biosensors and Bioelectronics*, 71 (2015) 476.
30. Q. Zhu, J. Zhang, Q. Tang, K. Zhao, A. Deng and J. Li, *Journal of The Electrochemical Society*, 163 (2016) B352.
31. S. Samanman, A. Numnuam, W. Limbut, P. Kanatharana and P. Thavarungkul, *Anal. Chim. Acta.*, 853 (2015) 521.
32. F. Cincotto, G. Martínez-García, P. Yáñez-Sedeño, T. Canevari, S. Machado and J.M. Pingarrón, *Talanta*, 147 (2016) 328.
33. G. Liu, M. Qi, Y. Zhang, C. Cao and E. Goldys, *Anal. Chim. Acta.*, 909 (2016) 1.
34. Y. Zhao, B. Trewyn, I. Slowing and V. Lin, *Journal of the American Chemical Society*, 131 (2009) 8398.
35. S. Sun, H. Zeng, D. Robinson, S. Raoux, P. Rice, S. Wang and G. Li, *Journal of the American chemical society*, 126 (2004) 273.

36. S. Ge, X. Jiao and D. Chen, *The Analyst*, 137 (2012) 4440.
37. S. Radhakrishnan, K. Krishnamoorthy, C. Sekar, J. Wilson and S.J. Kim, *Appl. Catal. B-Environ.*, 148 (2014) 22.
38. F. Yang, Z. Yang, Y. Zhuo, Y. Chai and R. Yuan, *Biosensors and Bioelectronics*, 66 (2015) 356.
39. D. Du, X. Xu, S. Wang and A. Zhang, *Talanta*, 71 (2007) 1257.
40. J. Lin, F. Yan, X. Hu and H. Ju, *Journal of Immunological Methods*, 291 (2004) 165.
41. D. Du, F. Yan, S. Liu and H. Ju, *Journal of immunological methods*, 283 (2003) 67.
42. B. Gu, C. Xu, C. Yang, S. Liu and M. Wang, *Biosensors and Bioelectronics*, 26 (2011) 2720.
43. Y. Zhuo, R. Yuan, Y. Chai and C. Hong, *The Analyst*, 135 (2010) 2036.

© 2017 The Authors. Published by ESG (www.electrochemsci.org). This article is an open access article distributed under the terms and conditions of the Creative Commons Attribution license (<http://creativecommons.org/licenses/by/4.0/>).